

Measuring the thermal expansion coefficient of tubular steel specimens with digital image correlation techniques

M. De Strycker^{a,*}, L. Schueremans^b, W. Van Paepegem^c, D. Debruyne^{a,d}

^a MeM2P research group, Catholic University College Ghent, Gebroeders Desmetstraat 1, B-9000 Ghent, Belgium

^b Department of Civil Engineering, KULeuven, Kasteelpark Arenberg 40, B-3001 Heverlee, Belgium

^c Department of Materials Science and Engineering, Ghent University, St.-Pietersnieuwstraat 41, B-9000 Ghent, Belgium

^d Department MTM, KULeuven, Kasteelpark Arenberg 44, B-3001 Heverlee, Belgium

ARTICLE INFO

Article history:

Received 16 December 2009

Received in revised form

3 March 2010

Accepted 19 May 2010

Available online 2 June 2010

Keywords:

Coefficient of thermal expansion

Digital image correlation

Steel

Tube

ABSTRACT

In this contribution it is investigated whether it is possible to measure the coefficient of thermal expansion (CTE) of steel with the aid of the digital image correlation (DIC) technique. DIC is first used to obtain reference values of the CTE of well-known steels (S235 and SS304) on simple geometries (rectangular blocks) within a low temperature interval (up to 120 °C). Although the strains that occur in this process are small, the CTE can be determined with good accuracy if enough images are available. The influence of the different parameters that control the correlation process showed no influence on the results. The values for the CTE are compared to available literature references and strain gauge measurements. The technique is extended to measure within a higher temperature interval (up to 600 °C), three-dimensional geometries (tubular samples), and a third material (SS409). It is shown that also in these cases, the results obtained are reliable. This contribution is part of a larger research effort predicting the residual stress in tubes coming from the welding process with finite element (FE) simulation. The goal of this research is therefore twofold: firstly obtaining the CTE in function of temperature, which can be used as input for the FE simulations; and secondly exploring the possibilities of measuring small thermal strains with DIC.

© 2010 Elsevier Ltd. All rights reserved.

1. Introduction

In order to measure the coefficient of thermal expansion (CTE) of a material, several well established methods are available, such as dilatometer tests, interferometry [1] and strain gauge measurements [2–4]. Although a dilatometer test can measure the CTE up to very high temperatures, it has the important drawbacks that the sample needs to be carefully prepared and that the test can only be performed on certain straightforward geometries. Measurements on tube specimens, for example, are generally not possible. It is also not straightforward to prepare test specimens for dilatometer tests from the tubes under consideration in this research due to the small wall thickness (2 mm) and the small radius of curvature (30 mm). Strain gauge measurements on the other hand can be performed on arbitrary geometries. The thermal strains arising in the material can be accurately determined if sufficient attention is paid to corrections stemming from differences in the CTE of the strain gauge and sample, the exact strain state at the location of the strain gauge and thermal compensation of the strain gauge itself. Unfortunately, these

measurements are limited to temperatures up to about 120 °C with standard strain gauges.

In this contribution it is investigated whether it is possible to measure accurately thermal strains and, hence, the CTE in tubular steel specimens up to 600 °C using digital image correlation (DIC) techniques [5–7]. Compared to both strain gauge measurements and dilatometer tests a DIC setup has the important advantage that it is a noncontact method. Furthermore, it is also possible to perform the measurements on arbitrary geometries as long as care is taken that the sample is free to stretch while heating or free to contract while cooling, since the derivation of the CTE from measured thermal strains relies on this observation. The preparation of the specimen is also minimal; a surface layer of white paint is applied to the zone of interest after which a random black paint speckle pattern is attached. In theory, DIC measurements have no limits on the temperatures and/or strains that can be reached, but practical boundary conditions, as discussed further on, limit the measuring process to ca. 600 °C.

It is a well established fact that small strains cannot be as precisely measured with DIC compared with e.g. strain gauges. In the application discussed here, typical strains vary in the range of 100–1000 μm/m, and large noise is to be expected during the measurements. Although there is a considerable amount of literature available on measuring small strains with DIC, there is

* Corresponding author. Tel.: +32 9 2658615; fax: +32 9 2658648.
E-mail address: maarten.destrycker@kahosl.be (M. De Strycker).

Table 1
Chemical composition of SS409 steel.

Element	C	Si	Mn	P	S	Cr	Mo	Ni	V	Cu	Ti
Weight%	0.019	0.421	0.234	0.023	0.007	11.916	0.004	0.097	0.048	0.052	0.162

no consensus about the accuracy that can be obtained during a particular experiment. For example, in Ref. [8] where plastic strains in steel and elastic strains in composite materials are measured, it is simply stated that DIC is especially suitable for large deformations ($> 0.1\%$). Tung et al. [9] compare DIC results in a tensile test on a low carbon steel sample with an electrical strain gauge measurement for strains up to $1600 \mu\text{m}/\text{m}$. From this they conclude that the DIC measurement has an accuracy of 0.04% . On the other hand, Hild and Roux [10], doing a so-called Brazilian disk test on a circular disk made of polycarbonate and submitted to diametrical compression, mention that the strain uncertainty, under certain conditions, can be as high as $2000 \mu\text{m}/\text{m}$, which is larger than their measured mean value of $1500 \mu\text{m}/\text{m}$. Amodio et al. in Ref. [11] obtain a strain sensitivity between 20 and 500 microstrains when performing tensile tests up to 2.5% strain on 6061 aluminium samples. Ivanov et al. [12] in their experiments on textile composite, measured noise of the order of about 0.05% for applied strains up to 0.7% . Finally, Fayolle et al. [13] obtain with their CORELLI^{CONTROL} a strain uncertainty of $10 \mu\text{m}/\text{m}$ with a zone of interest of 64 pixels and a gauge length L_0 of 400 pixels. These are a rather large subset size and a large gauge length, which are practically not achievable in the setup used in the research presented here. With a subset size of 55 pixels and L_0 of 110 pixels (values more appropriate to the case studied in this paper), a standard strain uncertainty of $100 \mu\text{m}/\text{m}$ could be obtained following [13], which is still rather large.

This lack of accuracy appears, at first, the most important drawback of the technique for this specific application. However, it will be shown further on that this noise can be quite easily filtered out if sufficient experimental data are collected. A similar procedure—using much less experimental data—was recently carried out by Bing et al. [14] to measure the CTE of polyimide (PI) composite film (which has a CTE of about $20 \mu\text{m}/\text{m}^\circ\text{C}$) between 20 and 140°C using DIC. In order to validate their approach they determined the CTE of a pure copper sample. They arrived at a value for the CTE of about 16.58 – $16.81 \mu\text{m}/\text{m}^\circ\text{C}$, and from this experiment it was concluded that their method is valid and could be used for measuring the thermal expansion of films as well. They state that the CTE of the PI film can be determined with a precision of about $1.33 \mu\text{m}/\text{m}^\circ\text{C}$.

The CTE α_m is generally obtained via $\varepsilon_{th} = \alpha_m(\theta) \cdot \Delta\theta$ in which ε_{th} is the measured thermal strain caused by a temperature difference $\Delta\theta$. In general, the CTE is a function of temperature, but for most materials it can be considered a constant in a large temperature range. It is essential for experimentally determining the CTE using traditional techniques that the thermal strain field within the sample is as homogeneous and uniform as possible, requiring both a uniform temperature during heating or cooling and no mechanical restraints on the sample, either external or internal, such that no stresses arise in the body during contraction or expansion. In principle, it is also possible to measure non-homogeneous thermal strain fields with a DIC setup. If these measured strain fields are combined with a numerical model of the setup in an inverse method, it should also be possible to derive a CTE from these kind of experiments. This is, however, beyond the scope of the present paper, but will be explored in forthcoming publications.

The approach in this contribution is split into two parts. In a first step the CTE of two common materials is studied by

measurements performed on a simple geometry. Both strain gauge and DIC measurements are performed in order to validate the DIC approach. The materials under study are a block of S235 ferritic steel and a block of SS304 austenitic stainless steel. In this section the experimental setup is outlined, the DIC procedure is explained and an assessment of the error on the obtained CTE is made. In a second part the CTE on a tubular specimen made of SS409 ferritic steel is measured up to temperatures of 600°C . This is done on both a flattened section of the tube and on the tube itself.

The research discussed in this contribution is part of a larger research effort predicting the residual stress in SS409 tubes coming from the welding process with finite element (FE) simulation. The alloy elements and their weight percentage in this stainless steel are mentioned in Table 1. The tubes under consideration in this research have not undergone any heat treatments. The goal of the research described here is twofold: firstly obtaining the CTE in function of temperature, which can be used as input for the FE simulations; and secondly exploring the possibilities of measuring small thermal strains with DIC.

2. Validation of the DIC approach

In order to demonstrate the validity of the DIC approach, two sets of experiments were performed on both a S235 and a SS304 steel block. In a first step the CTE is measured with both strain gauges and DIC for temperatures up to 120°C , in which the effects of using different settings for the DIC processing are investigated. It is shown that the DIC procedure yields similar values as the strain gauge measurements for the derived CTE. Next, DIC measurements are taken up to temperatures of 600°C . Results are compared to values reported in literature.

2.1. Experimental setup

The S235 steel block ($40 \times 66 \times 17 \text{ mm}$) is first annealed to minimize effects of residual stresses. A K-type thermocouple is put in a hole in the middle of the block. Two strain gauges are glued to the back and front surface of the specimen. This was done in order to verify that the sample was indeed free to expand or contract and that no bending stresses occurred. The strain gauges used were linear strain gauges with a measuring grid length of 6 mm , a resistance of 350Ω and compensated for a material with a CTE of $16 \mu\text{m}/\text{m}^\circ\text{C}$. Next, a uniform white paint layer was applied to the specimen, followed by a random black speckle pattern as is usual in this procedure. The speckle size varied between ca. 0.1 and 0.8 mm . A similar procedure was followed for the SS304 steel block ($92 \times 100 \times 8 \text{ mm}$).

The DIC procedure was carried out using two cameras. It could be argued that one camera should be sufficient to perform the measurements, since the specimens studied are flat, and the out-of-plane displacements are very small. This was not done since the same setup was used to measure the strains on the tubular specimen which requires a 3D view. The camera setup is shown in Fig. 1. Both cameras are focussed on the area of interest, i.e. the plane of the speckle pattern on the object. In this setup one pixel corresponds to a physical dimension of $84 \mu\text{m} \times 84 \mu\text{m}$. In order to ensure good lighting conditions and small exposure times

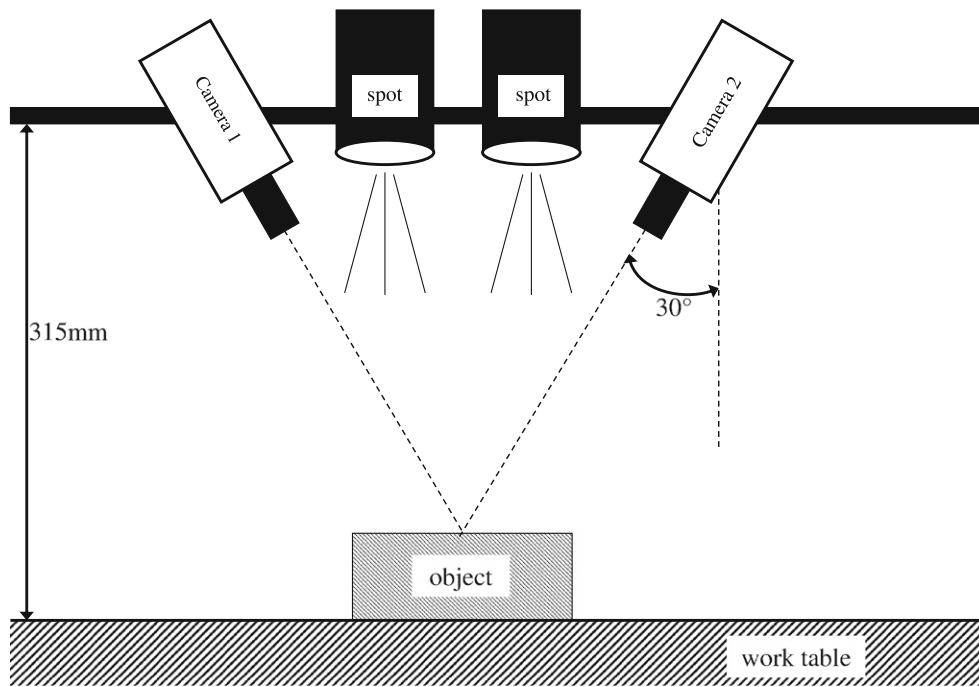


Fig. 1. Schematic setup of the DIC experiment.

(about 6–10 ms) three light sources were used: two intense one between the cameras and one larger, diffuse source above the cameras.

In the first series of tests both samples are heated up to 120 °C in an oven and then placed under the cameras. Images are taken every second while the sample is radiating and convecting its heat to the surrounding environment at room temperature. As the specimen is cooling down, the temperature differential between the environment and the sample is reduced. The sampling rate of the cameras was also adjusted. On average, an image is taken within each temperature interval of 1 °C. As the light sources create a lot of heat near the specimen, the actual room temperature monitored around the specimen was 45 °C. While the DIC measurements are limited to the cooling step, with the strain gauges the heating phase can be measured as well. Below 45 °C, the strain gauge measurement can go on with the light sources switched off. This further decreases the ambient temperature to about 25 °C and allows the strain gauge measurements to extend over a larger temperature interval.

In order to allow for the free expansion of the sample, no clamping whatsoever was used. This allows the specimens not only to deform, but also to move as a rigid body. Rigid body motions can occur because the worktable has a polished surface minimising the friction between the object and the surface. An accidental small external force caused by e.g. the stiff thermocouple wires can disturb the sample. These rigid body motions are assumed to be small, but, in any case, they are not relevant since they are removed from the DIC procedure when calculating strains from the measured displacement fields.

In the second series of experiments where the specimens are heated to 600 °C, the strain gauges were removed from the samples. The maximum temperature of 600 °C was dictated by three practical limitations. First, at around these temperatures the white surface layer turns slightly yellow, because the steel underneath starts glowing, while the initially black speckles turn grey. This results in a change of the grey values of the images taken which in turn, when processed by the DIC procedure, creates artificial displacements and strains, since this procedure

relies, amongst other things, on the grey value interpolation of the pixels within each image. Second, the paint that is used is based on polyester resin. The manufacturer of this paint limits its use to 650 °C [15]. Third, due to convection of the air surrounding the hot specimen, the images taken become increasingly blurred, hampering the reliability of the pattern-matching algorithm. While the third limitation could be avoided by creating a laminar air flow between the object and the cameras, for the first two limitations no alternatives are presently available.

2.2. Strain gauge measurements

Strain gauge producers (HBM [4], Vishay [2]) provide technical notes which describe how to measure thermal expansion of materials. Although the procedures may look different at first sight, they are based on the same principle: the strain measured with the strain gauges on the material under investigation is compared to the strain measured on a reference material. In Finke et al. [2,3] the reference material has a very low CTE (e.g. Invar), whereas in [4], the well-known CTE of the strain gauge is taken as a reference value. The latter method avoids measuring thermal strains on a second (very specific) material.

When using strain gauges for strain measurement under varying temperature conditions, apparent strains ε_a are measured [4]:

$$\varepsilon_a = \varepsilon_m + \varepsilon_s + (\alpha_m - \alpha_{SG}) \cdot \Delta\theta \quad (1)$$

in which ε_a is the apparent strain, indicated by the amplifier, ε_m the strain triggered by the mechanical load (zero in these experiments), ε_s the apparent strain of the strain gauge without mechanical strain, known as a function of temperature for each strain gauge, α_m the CTE of the measured object, α_{SG} the CTE of the strain gauge (in these experiments 16 $\mu\text{m}/\text{m}^\circ\text{C}$), and $\Delta\theta$ the temperature interval over which the strain is measured. When the mechanically induced strain (ε_m) is zero, formula (1) is analogous to the formula used in [2]. From formula (1) the thermal strains, and thus the CTE of the material under investigation can be calculated.

A typical plot of the apparent measured strain and the corrected thermal strains obtained from such a measurement is shown in Fig. 2 for the S235 steel block. The lower part of the curve corresponds to the heating of the specimen, while the upper part corresponds to the cooling step. Although care was taken to reduce the hysteresis effect that is always present in strain gauge measurements due to non-uniform heating and cooling [16], there is still a difference between tensioning (heating) and compressing (cooling) the strain gauge. The temperature range is limited by the glue used, which is a cyanoacrylate adhesive that has a guaranteed durability up to 120 °C and a softening point of 165 °C. Together with the fact that the apparent strain ε_s is known up to 120 °C, this sets the practical limit for strain gauge measurements at 120 °C. As expected, the actual strain–temperature curve is almost perfectly linear. A constant CTE can then be defined as the slope of the straight line through the collected data points. Table 2 presents the results for both materials, measured during heating and during cooling. It is clear that differences are small and for the S235 steel an average value of $11.618 \mu\text{m}/\text{m}^\circ\text{C}$ for the CTE can be assumed, while for SS304 the average results is $16.55 \mu\text{m}/\text{m}^\circ\text{C}$. These values will serve as a reference for the values obtained with the DIC procedure. The 99% confidence interval, defined as three times the standard deviation, is also mentioned for the values.

When researching literature for the CTE of S235, values ranging from 11.5 to $14 \mu\text{m}/\text{m}^\circ\text{C}$ are found [1,17,18] while for SS304 values ranging from 16 to $20 \mu\text{m}/\text{m}^\circ\text{C}$ can be found [17–21]. Certainly, both of the measured CTE's lie within these ranges. More importantly, the cited textbook values for the CTE of both materials show that an exact measurement of the CTE is mandatory if its value is to be used in calculations where thermal

expansion plays an important role (e.g. as used in determining the residual stresses in welding simulations).

2.3. DIC measurements

2.3.1. DIC measurements up to 120 °C

The DIC measurements on the two steel blocks were only performed during the cooling of the specimens, since practical limitations made it impossible to photograph the specimen while being heated in the oven. As a result, in the first image taken, the temperature is highest, while the last image in the set shows the sample at room temperature, i.e. 45 °C. For all samples, one image is taken every second between 120 and 65 °C, while from 65 °C to room temperature, only every 15 s an image was taken, because of the lower strain rates occurring at lower temperature differentials. Next, from these images the displacement fields are obtained via correlation, and the strains derived using the Vic3D software from Correlated Solutions. For the actual displacement calculation a normalized-sum-of-squared-differences (NSSD) correlation algorithm with cubic B-spline interpolation, a subset of 55 pixels (px) and a step size of 3 px are used, unless otherwise specified. Next the obtained displacements are smoothed via a so-called strain window method. This is a commonly adopted technique during the process of strain derivation [22–25]. This analytical approximation makes the calculation of the full-field strain information straightforward. In this research a default strain window of 5 is used. This means that the displacement field is smoothed over an area of 5×5 displacement data points. Taking into account the step size and the dimension of one pixel, this leads to strain gauge surface of about $1 \text{ mm} \times 1 \text{ mm}$. The

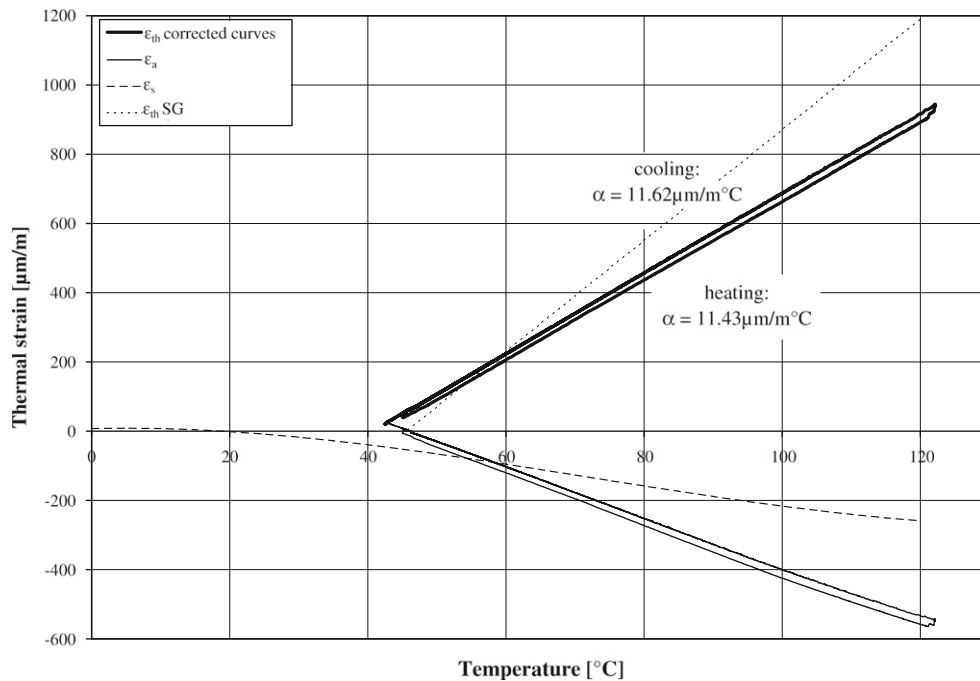


Fig. 2. Typical result of a strain gauge measurement with indication of ε_a and $\varepsilon_{th,SG} = \alpha_{SG} \cdot \Delta\theta$. Example with $\theta_0 = 46^\circ\text{C}$ and $\Delta\theta = 76^\circ\text{C}$.

Table 2

Coefficients of thermal expansion of S235 and SS304 as obtained using strain gauge measurements.

Steel	θ_0 (°C)	$\Delta\theta$ (°C)	CTE-heating ($\mu\text{m}/\text{m}^\circ\text{C}$)	99% conf. int. ($\mu\text{m}/\text{m}^\circ\text{C}$)	CTE-cooling ($\mu\text{m}/\text{m}^\circ\text{C}$)	99% conf. int. ($\mu\text{m}/\text{m}^\circ\text{C}$)
S235	36	79	11.660	0.006	11.575	0.001
SS304	51	41	16.60	0.01	16.50	0.02

strains calculated in the Vic3D-software are Green–Lagrange strains. The effect of changing the correlation settings and strain window size on the identified CTE is discussed in Section 2.4.

As already noted in the introduction, the measurement of very small displacements and strains using DIC is not easy because of the expected noise that can be very substantial. One way to deal with this problem is to average the measured strains over a large area (dubbed the area of interest (AOI)) where the strains are supposed to be homogeneous. Therefore, an area as large as possible on the specimen was selected to calculate the strains. It measured 24 × 38 mm and contained approximately 130 000 px. With the step size and strain window size mentioned above, this leads to about 5760 points where strains are calculated. Although the thermal strain is supposed to be homogeneous in the area of interest, the scatter on the measured strains in one image is substantial. Fig. 3 shows the distribution of the ϵ_{xx} strain in one such image. This image was taken at 121 °C on the S235 steel

block. Results for other strain components and images at other temperatures are similar.

The noise on the measured strains can be considered approximately normally distributed, as shown in Fig. 3. Therefore, the mean value of all calculated strains is taken as the thermal strain corresponding to the temperature at which the image was taken. The mean value of the strain distribution shown in Fig. 3 is 913 $\mu\text{m}/\text{m}$ while the standard deviation on this mean value is 591 $\mu\text{m}/\text{m}$. The standard deviation is slightly smaller for images at lower temperatures. It is exactly this large standard deviation that can cause doubt about the usability of DIC for small strain measurements as mentioned in the introduction. This is a valid observation if only one image is considered, but when a large number of images is taken into account, these uncertainties are substantially reduced, as will be shown below.

A typical result of thermal strain versus temperature obtained in the manner mentioned above is shown in Fig. 4 for the S235

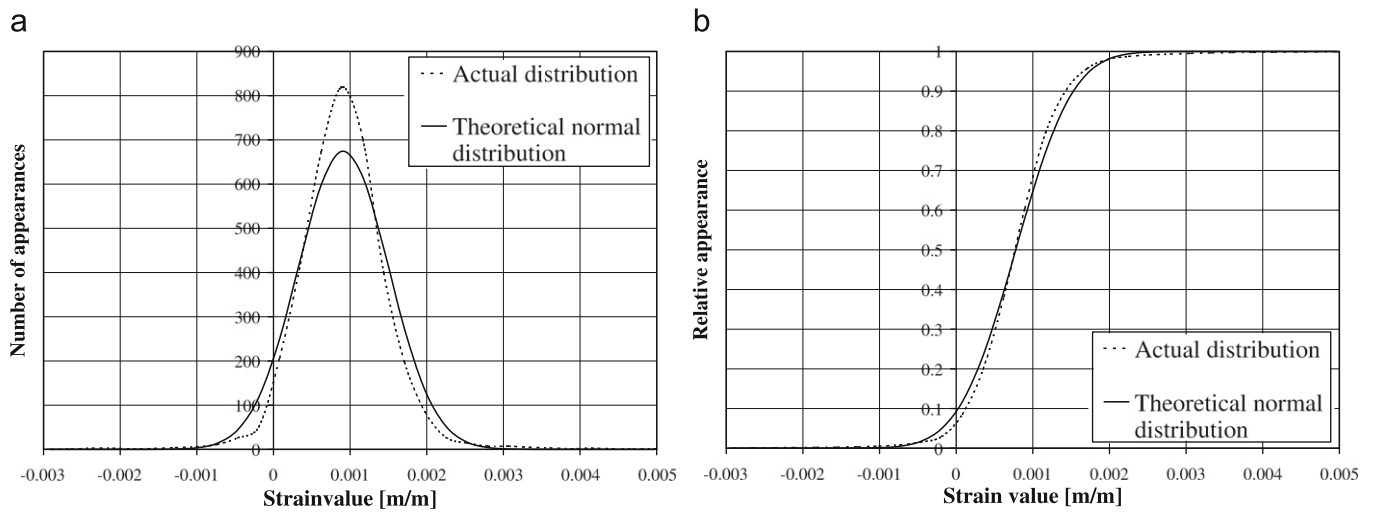


Fig. 3. Strain distribution of ϵ_{xx} over one image: (a) comparison with normal distribution with the same mean (913 $\mu\text{m}/\text{m}$) and standard deviation (591 $\mu\text{m}/\text{m}$), (b) comparison of the cumulative strain distribution. Image taken from the S235 experiment at 121 °C.

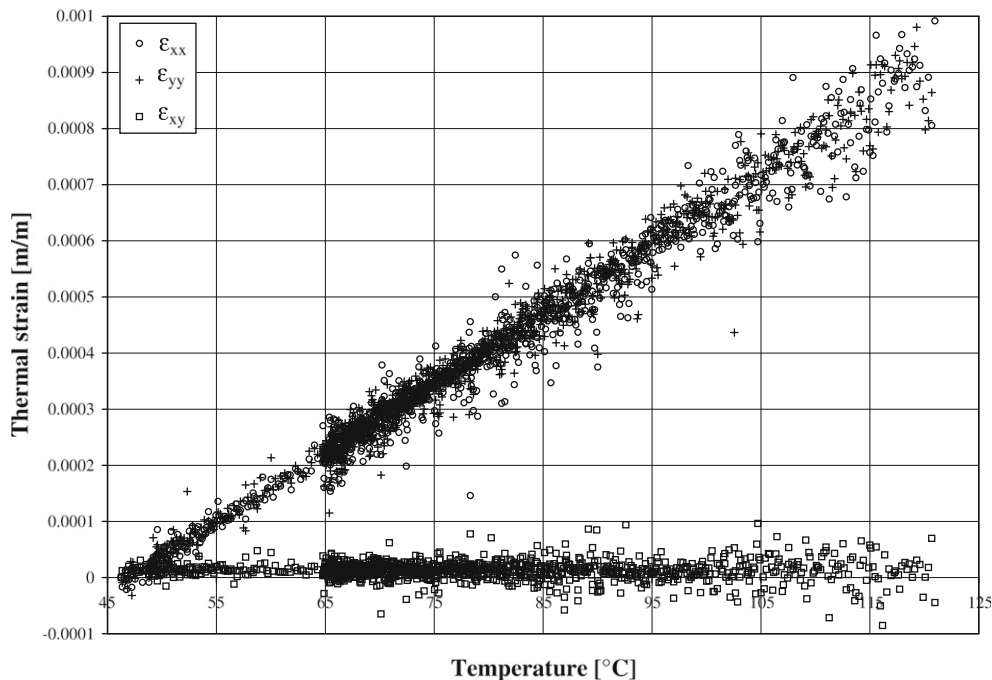


Fig. 4. Typical thermal strain vs temperature graph from DIC measurement for S235 steel block.

steel block. Both in-plane normal strains (ϵ_{xx} and ϵ_{yy}) and the shear strain (ϵ_{xy}) are shown. As expected the strains in the x and y direction are similar while the measured shear strain equals zero on average since the specimen is free to expand/contract without any restrictions. From these strain–temperature curves, a linear fit of the slope of the curve was performed yielding the coefficient of thermal expansion. Linear regression analysis leads to a CTE of $12.3 \mu\text{m}/\text{m}^\circ\text{C}$ with a 99% variance of $0.2 \mu\text{m}/\text{m}^\circ\text{C}$ for the S235 sample and $17.1 \mu\text{m}/\text{m}^\circ\text{C}$ with a 99% variance of $0.3 \mu\text{m}/\text{m}^\circ\text{C}$ for the SS304 sample. This illustrates that although the standard deviation in one image may be large compared to the mean value of the strain, the uncertainty on the measured CTE is much smaller if it can be assumed that the CTE is constant within this temperature range.

The CTE values found with DIC are slightly higher than those found with strain gauge measurements, but still well in the range quoted by literature (see Section 2.2). Although the variance on the values from the DIC measurements are larger, the uncertainty is very acceptable. This part of the research shows that although the measured strains are small compared to other typical DIC applications, and although the noise on the strains within one image is high, by taking enough images, it is possible to keep the variance on the thermal strain versus temperature low and to find results in good agreement with the strain gauge measurements. Having thus established the usability of the DIC approach for low temperatures and correspondingly low strains, the use in higher temperature range can be explored. Since at higher temperatures the strains are proportionally higher, it is reasonable to assume that the relative variance on the strains will be smaller, yielding even more accurate measurements.

2.3.2. DIC measurements up to 600 °C

Again tests were performed for both S235 and SS304, this time for temperatures up to 600 °C. A typical result for the measured thermal strain versus temperature is shown in Fig. 5 for the S235 sample. It is well known that the CTE is slightly higher for higher temperatures, and by analogy with Eurocode 3 [17] it is assumed that the thermal strain varies with temperature in a quadratic

fashion:

$$\epsilon_{th} = a \cdot (\theta - \theta_0)^2 + b \cdot (\theta - \theta_0) + c \tag{2}$$

or for the data shown in Fig. 5:

$$\epsilon_{th} = 4.7 \times 10^{-3} \mu\text{m}/\text{m}^\circ\text{C}^2 \cdot (\theta - \theta_0)^2 + 12.5 \mu\text{m}/\text{m}^\circ\text{C} \cdot (\theta - \theta_0) - 2 \times 10^1 \mu\text{m}/\text{m} \tag{3}$$

with, for this particular experiment, $\theta_0 = 49^\circ\text{C}$. From this fit one can see that the linear term is in good agreement with the former derived linear fit for the lower temperature interval. It can also be verified that the identified coefficients of the quadratic term and the linear term are in agreement with the values cited in Eurocode 3. The difference of the constant value can be attributed to the different reference temperature (49°C in this research and 20°C in Eurocode 3). Table 2 gives an overview of the identified values for both in-plane orientations.

From Table 3 it is clear that the linear coefficient is almost not affected by being determined over a larger temperature interval. The quadratic coefficient displays a standard deviation which is approximately 10% of its value, which means that the value as such can be used. The standard deviation on the constant term is larger than the value itself, but this value is small enough to be neglected. In a similar way, a quadratic expression was fitted to the

Table 3
Coefficients of the quadratic function of thermal expansion of S235 and SS304.

	a ($\mu\text{m}/\text{m}^\circ\text{C}^2$)	99% conf. int. ($\mu\text{m}/\text{m}^\circ\text{C}^2$)	b ($\mu\text{m}/\text{m}^\circ\text{C}$)	99% conf. int. ($\mu\text{m}/\text{m}^\circ\text{C}$)	c ($\mu\text{m}/\text{m}$)	99% conf. int. ($\mu\text{m}/\text{m}$)
S235						
ϵ_{xx}	4.7E-03	0.5E-03	12.5	0.3	-2E+01	3E+01
ϵ_{yy}	4.3E-03	0.3E-03	12.5	0.2	-1E+01	2E+01
SS304						
ϵ_{xx}	3.9E-03	0.8E-03	18.4	0.4	-6E+01	4E+01
ϵ_{yy}	3.7E-03	0.7E-03	18.5	0.3	-6E+01	3E+01

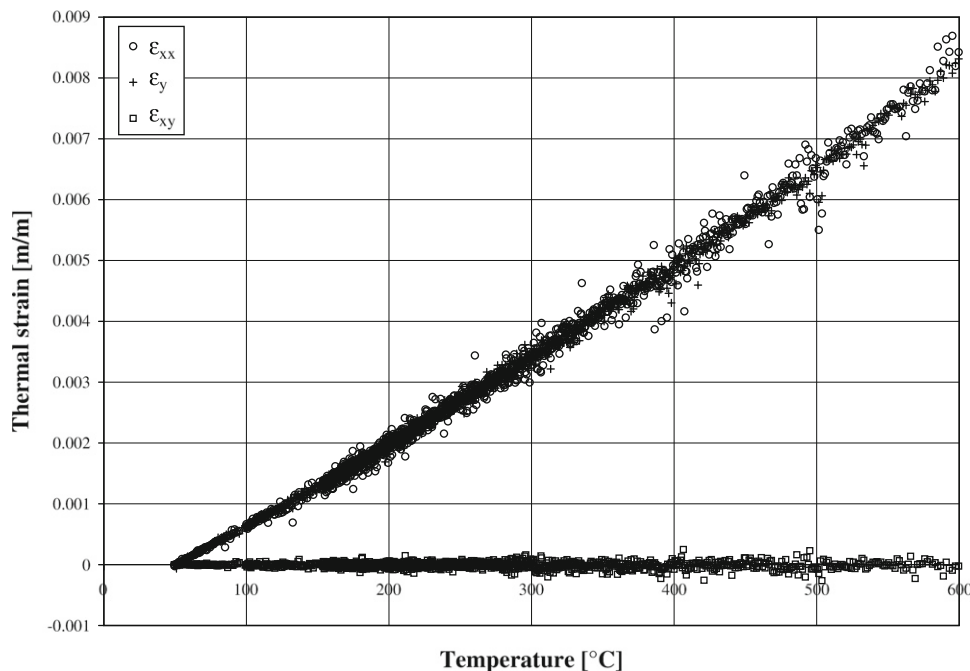


Fig. 5. Thermal strains (ϵ_{xx} , ϵ_{yy} and ϵ_{xy}) for the S235 steel block for temperatures up to 600 °C.

SS304 data. The results are also presented in Table 3 (with $\theta_0 = 51^\circ\text{C}$). Here again the coefficient of the linear term is in agreement with the CTE found in the lower temperature interval, though it is somewhat higher. Similar remarks apply for the quadratic and constant coefficient. From this set of experiments on two types of steels with well known CTE and simple geometries it can be concluded that it is possible to measure the CTE of steels with the help of DIC sufficiently accurately up to 600°C .

2.4. Discussion of the DIC results

To assess the effect of using different subset and strain window sizes on the identified CTE, a sensitivity analysis on these parameters is performed for the S235 material for the CTE up to 120°C . The results of this analysis are summarized in Table 4. From this table it can be concluded that neither the subset size nor the strain window size has a significant influence on the results, the main reason being that the small step size used ensures that an average is calculated over many data points. Both the value found for the CTE and the variance on this value do not change significantly. This is within expectations as the strain field is assumed to be homogeneous. Potential differences arising from the choice of a correlation coefficient, the intensity interpolation

scheme and the transformation order have not been investigated as its effects are well understood [26,27]. The NSSD correlation coefficient in conjunction with bicubic intensity interpolation and an affine subset transformation are adopted in order to reduce systematic errors.

At the same time, the effect of choosing a smaller area of interest (AOI) over which the strains are averaged was also investigated. As the strain field is expected to be homogeneous, one could average the strain in one image over as many values as possible, but at the borders of the AOI, edge effects may occur. Three regions were compared: the strains were averaged (A) over all pixels in which the strains were calculated; (B) over a region leaving out the boundaries (see Fig. 6(a)); and (C) over a region in the middle of the area where results are available (see Fig. 6(b)). Region (C) was selected to check the effect of taking significantly fewer points for the strain calculation. The results of these calculations are also included in Table 4. From this table it can be seen that there is not much difference between averaging the strain over all points, and region (B). This means that the edge effects do not affect the strain value obtained for one image. For region (C) the standard deviation is systematically higher, although the identified CTE is not significantly different. The straightforward conclusion here is that the larger the region over which the strains are averaged, the smaller the variance on the CTE will be [25].

Table 4

Influence of the subset size and the strain window (SW) size on the CTE of S235 in the low temperature interval, obtained for ϵ_{xx} .

Subset (px)	Step (px)	SW (-)	All values		Region B		Region C	
			CTE ($\mu\text{m}/\text{m}^\circ\text{C}$)	99% conf. int. ($\mu\text{m}/\text{m}^\circ\text{C}$)	CTE ($\mu\text{m}/\text{m}^\circ\text{C}$)	99% conf. int. ($\mu\text{m}/\text{m}^\circ\text{C}$)	CTE ($\mu\text{m}/\text{m}^\circ\text{C}$)	99% conf. int. ($\mu\text{m}/\text{m}^\circ\text{C}$)
9	5	5	12.4	0.1	12.3	0.2	12.4	0.3
17	5	5	12.2	0.1	12.2	0.2	12.3	0.3
25	5	5	12.2	0.1	12.2	0.2	12.2	0.3
35	3	5	12.2	0.2	12.1	0.2	12.3	0.3
55	3	5	12.1	0.2	12.1	0.2	12.2	0.3
55	3	5	12.1	0.2	12.1	0.2	12.1	0.3
55	3	11	12.1	0.2	12.1	0.2	12.2	0.3
55	3	17	12.1	0.2	12.1	0.2	12.2	0.3
55	3	25	12.1	0.2	12.1	0.2	12.2	0.3

Values are averages of all strain values, a large area (see Fig. 6(a)) and a smaller area (see Fig. 6(b)).

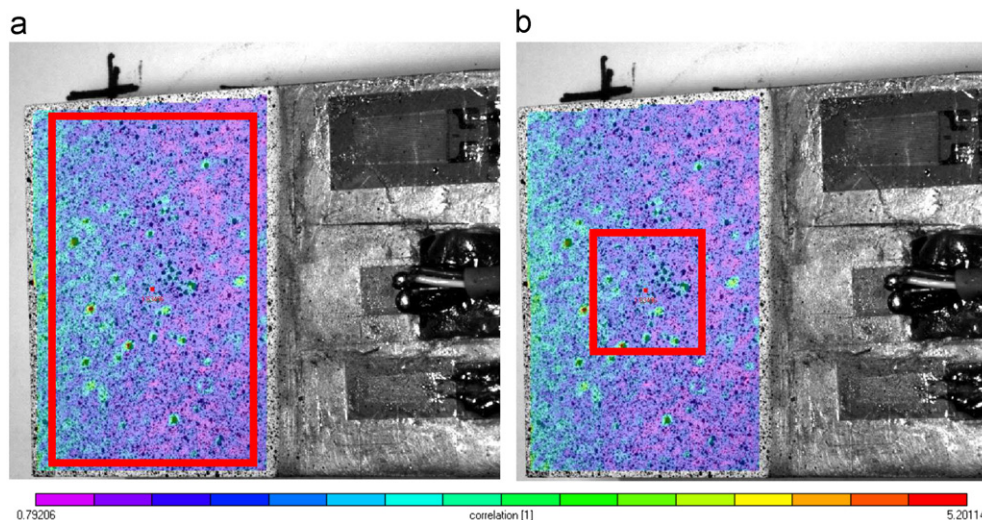


Fig. 6. Correlation result on the S235 steel block: the lower the value for the correlation error, the better the correlation. The area of interest (AOI) is taken as the whole area with the speckle pattern. Data (displacements, strains and correlation results) are available in a reduced area related to the subset size. The resulting strain is averaged over the area for which data are available (a) region (B): leaving out the points in the boundary; (b) region (C) only points in the middle of the AOI.

3. Measurement of the CTE of a tubular specimen using DIC

3.1. Experimental setup

Two types of experiments were carried out to determine the coefficient of thermal expansion of a ferritic SS409 tubular sample with a diameter of 60 mm and a wall thickness of 2 mm. First a sample was cut from a tube and flattened as well as possible. On this flattened sample two strain gauges were attached perpendicular to one another in order to measure a potential anisotropy in the thermal strains in the circumferential and longitudinal direction. As the small tube thickness does not allow the thermocouple to be put inside the material, it was spot welded onto the surface of the object. Secondly a tubular sample was also fitted with two strain gauges; one in the longitudinal and the other in circumferential direction. A thermocouple was spot welded onto the outer surface of the tubular specimen and positioned between the two strain gauges. To prevent rolling or moving of the tube, it was placed in a steel block with a V-groove. As before, validation measurements using strain gauges were performed up to 120 °C. The thermal strains and the CTE were determined in exactly the same fashion. For the DIC measurements, care was taken in choosing the area of interest such that this area was in good view of both cameras, yielding low correlation errors. After these validation experiments, the tube was heated to 600 °C in order to determine the variation of its CTE with temperature.

3.2. Strain gauge measurements

The results of the strain gauge measurements on the flattened sample are given in Table 5 for three separate experiments. Preferential directions may exist in the tubular material, leading to an anisotropic CTE. Therefore the CTE was measured in both hoop and longitudinal direction. However, in the strain gauge measurements on the flattened tube samples no clear anisotropic effects in the CTE are noticed. A similar observation holds for the tubular samples (Table 6) where the differences between the identified CTE are small, especially because extra care should be taken when using the compensation curves (ϵ_s in formula (1)) when the strain gauge is used on a curved surface. This makes it difficult to judge whether the small differences found are

Table 5
Coefficients of thermal expansion of SS409 flattened tube sample as obtained using strain gauge measurements.

θ_0 (°C)	$\Delta\theta$ (°C)	CTE ϵ_{xx} heating ($\mu\text{m}/\text{m} \cdot \text{C}$)	CTE ϵ_{xx} cooling ($\mu\text{m}/\text{m} \cdot \text{C}$)	CTE ϵ_{yy} heating ($\mu\text{m}/\text{m} \cdot \text{C}$)	CTE ϵ_{yy} cooling ($\mu\text{m}/\text{m} \cdot \text{C}$)
28	68	10.8	10.3	10.1	10.4
37	65	10.3	10.3	10.4	10.2
30	86	10.6	10.3	9.3	9.9

99% confidence intervals are of the same order as for S235 and SS304 samples.

Table 6
Coefficients of thermal expansion of SS409 tubular sample as obtained using strain gauge measurements.

θ_0 (°C)	$\Delta\theta$ (°C)	CTE ϵ_{xx} heating ($\mu\text{m}/\text{m} \cdot \text{C}$)	CTE ϵ_{xx} cooling ($\mu\text{m}/\text{m} \cdot \text{C}$)	CTE ϵ_{yy} heating ($\mu\text{m}/\text{m} \cdot \text{C}$)	CTE ϵ_{yy} cooling ($\mu\text{m}/\text{m} \cdot \text{C}$)
23	85	11.0	10.2	10.0	9.4
24	81	10.5	10.3	10.1	9.6
23	84	11.1	10.5	11.1	10.5

Standard deviations are of the same order as for S235 and SS304 samples.

Table 7

Coefficients of thermal expansion of SS409 flattened tube samples as obtained using DIC measurements.

θ_0 (°C)	$\Delta\theta$ (°C)	CTE ϵ_{xx} ($\mu\text{m}/\text{m} \cdot \text{C}$)	99% conf. int. ($\mu\text{m}/\text{m} \cdot \text{C}$)	CTE ϵ_{yy} ($\mu\text{m}/\text{m} \cdot \text{C}$)	99% conf. int. ($\mu\text{m}/\text{m} \cdot \text{C}$)
28	68	11.0	0.2	11.4	0.2
30	86	10.3	0.2	10.3	0.2
55	40	10.7	0.4	10.8	0.2
32	69	10.4	0.2	10.4	0.2
35	64	10.3	0.4	10.5	0.5

significant or not. Textbook values for the CTE of this material range between 9.3 and 12 $\mu\text{m}/\text{m} \cdot \text{C}$ in the temperature interval 20–100 °C [1].

3.3. DIC measurements

In the DIC measurements on the flattened tube samples, no anisotropy was found in the low temperature experiments (Table 7) nor the high temperature interval. As before, the high-temperature behaviour is fitted with a quadratic relation between thermal strain and temperature:

$$\epsilon_{th,xx} = 3.2 \times 10^{-3} \mu\text{m}/\text{m} \cdot \text{C}^2 \cdot (\theta - \theta_0)^2 + 10.5 \mu\text{m}/\text{m} \cdot \text{C} \cdot (\theta - \theta_0) + 6 \times 10^1 \mu\text{m}/\text{m}$$

$$\epsilon_{th,yy} = 2.7 \times 10^{-3} \mu\text{m}/\text{m} \cdot \text{C}^2 \cdot (\theta - \theta_0)^2 + 10.6 \mu\text{m}/\text{m} \cdot \text{C} \cdot (\theta - \theta_0) - 2 \times 10^1 \mu\text{m}/\text{m} \tag{4}$$

with $\theta_0 = 48$ °C. The values for the low temperature interval and the linear coefficients are in mutual agreement, and also compare well to the strain gauge measurements. The values for the CTE found with DIC in the lower temperature interval are closer to each other than those found with the strain gauges. A comparison with literature for the higher temperature intervals is difficult, as to the authors' knowledge, no curves for this particular steel are available.

As anisotropy in the CTE is not found in the flattened tube samples, neither is it expected in the tubular samples. However, to determine the CTE on the tubular section, out-of-plane deformations must be measured, which leads to higher standard deviations on the CTE. It was found, however, that the 99% confidence intervals are not noticeably higher than for the flattened tube section (Table 8). Again, the CTE in longitudinal direction is identical to that in circumferential direction.

A fit on the high temperature data resulted in the following strain versus temperature relation:

$$\epsilon_{th,xx} = 6.4 \times 10^{-3} \mu\text{m}/\text{m} \cdot \text{C}^2 \cdot (\theta - \theta_0)^2 + 9.3 \mu\text{m}/\text{m} \cdot \text{C} \cdot (\theta - \theta_0) + 3 \times 10^2 \mu\text{m}/\text{m}$$

$$\epsilon_{th,yy} = 5.9 \times 10^{-3} \mu\text{m}/\text{m} \cdot \text{C}^2 \cdot (\theta - \theta_0)^2 + 9.4 \mu\text{m}/\text{m} \cdot \text{C} \cdot (\theta - \theta_0) + 7 \times 10^1 \mu\text{m}/\text{m} \tag{5}$$

with in this case $\theta_0 = 50$ °C and $\Delta\theta = 500$ °C.

A second experiment yielded similar values:

$$\epsilon_{th,xx} = 7.4 \times 10^{-3} \mu\text{m}/\text{m} \cdot \text{C}^2 \cdot (\theta - \theta_0)^2 + 9.3 \mu\text{m}/\text{m} \cdot \text{C} \cdot (\theta - \theta_0) + 6 \times 10^1 \mu\text{m}/\text{m}$$

$$\epsilon_{th,yy} = 6.1 \times 10^{-3} \mu\text{m}/\text{m} \cdot \text{C}^2 \cdot (\theta - \theta_0)^2 + 9.6 \mu\text{m}/\text{m} \cdot \text{C} \cdot (\theta - \theta_0) + 3 \times 10^1 \mu\text{m}/\text{m} \tag{6}$$

with in this case $\theta_0 = 46$ °C and $\Delta\theta = 478$ °C.

Table 8

Coefficients of thermal expansion of SS409 tubular samples as obtained using DIC measurements.

θ_0 (°C)	$\Delta\theta$ (°C)	CTE ϵ_{xx} ($\mu\text{m}/\text{m}\cdot\text{C}$)	99% conf. int. ($\mu\text{m}/\text{m}\cdot\text{C}$)	CTE ϵ_{yy} ($\mu\text{m}/\text{m}\cdot\text{C}$)	99% conf. int. ($\mu\text{m}/\text{m}\cdot\text{C}$)
40	39	11.6	0.3	11.6	0.3
47	48	11.2	0.5	11.7	0.4
41	52	11.2	0.4	11.4	0.3

The identified coefficients of these four curves are in close agreement. Three remarks can be made about these high temperature curves. First, the coefficients of the linear term differ from the coefficients obtained from the low temperature interval, indicating a higher temperature dependence of this material compared to S235 and SS304. Second, the coefficient of the quadratic term is higher than that from the (ferritic) S235 steel; the same remark as above applies. Third, the constant coefficient is larger in absolute value, pointing to more noise in the measured strains. These three remarks lead to the conclusion that for SS409 material the CTE is more dependent on the temperature than for the other steels discussed in this paper. It is thus important to have the CTE in function of temperature for this ferritic stainless steel when accurate input is needed for FEA simulations.

Moreover it is shown that DIC can be used to measure homogeneous thermal strain fields on 3D objects and obtain from these the CTE of the material for temperatures up to 600 °C.

4. Conclusion and final remarks

In this research it has been shown that the coefficient of thermal expansion (CTE) of steel can be measured with the aid of the digital image correlation (DIC) technique. In other words it is possible to measure homogeneous thermal strain fields on steel samples with DIC. Although the strains are small for a low temperature interval and the variance on the strain calculated within one image is quite large, it is possible to determine the CTE with good accuracy if enough images are available. In this case one image within each temperature interval of 1 °C gave good results. The larger the area over which the strains are averaged in one image, the smaller the variance on the obtained CTE. The different parameters that control the correlation process showed no influence on the results. It is clear that this method will yield better results for materials with a larger CTE than the steels mentioned in this article, e.g. plastics (with a CTE of about 40–50 $\mu\text{m}/\text{m}\cdot\text{C}$) or rubber (with a CTE of about 70 $\mu\text{m}/\text{m}\cdot\text{C}$), as the thermal strains will be larger.

The CTE for all three steels (S235, SS304 and SS409) found with DIC is in agreement with available literature values. For measurements up to 120 °C the results are also in agreement with strain gauge measurements. The CTE in function of temperature can be considered as more appropriate as input for finite element simulations than the vague values suggested in literature.

Now that the thermal strains on three-dimensional objects, uniformly heated up to 600 °C can be measured using DIC, the possibilities of using this technique to measure thermal strains due to non-uniform heating and cooling cycles, i.e. welding, will be explored. In this case, the non-homogeneous strain fields can then be compared to strains calculated with finite element simulations. These residual strains can then be related to the residual stresses due to welding of cold-rolled steel tubes.

Acknowledgments

The authors would like to thank R. Van Hecke for helping with the sample preparation and J. Pumphrey for the language tips.

References

- [1] Cervera F, editor. ASM ready reference: thermal properties of metals. ASM International—The Materials Information Society, 2002.
- [2] Vishay Micro-Measurements. Measurement of thermal expansion coefficient using strain gages. Technical Note tn-513-1, <www.vishaymg.com> ; October 2007.
- [3] Finke T, Heberling T. Determination of thermal-expansion characteristics of metals using strain gages. *Experimental Mechanics* 1978;18(4):155–8.
- [4] HBM. Experimental stress analysis—correcting thermally induced strain during strain gage measurements, can strain gages be used to determine the thermal coefficient of linear expansion α of a given material?.
- [5] Sutton M, Wolters W, Peters W, Ranson W, McNeill S. Determination of displacements using an improved digital correlation method. *Image and Vision Computing* 1983;1:133–9.
- [6] Chu T, Ranson W, Sutton M, Peters W. Applications of digital image correlation techniques to experimental mechanics. *Experimental Mechanics* 1985;25(3):232–44.
- [7] Sutton M, Orteu J, Schreier H. *Image correlation for shape, motion and deformation measurements*. Springer: New York; doi:10.1007/978-0-387-78747-3.
- [8] Lecompte D. Elastic and elasto-plastic material parameter identification by inverse modeling of static tests using digital image correlation. PhD thesis, Royal Military Academy & Vrije Universiteit Brussel, Brussels, Belgium; 2007.
- [9] Tung S-H, Shih M-H, Kuo J-C. Application of digital image correlation for anisotropic plastic deformation during tension testing. *Optics and Lasers in Engineering*, doi:10.1016/j.oplaseng.2009.09.011.
- [10] Hild F, Roux S. Digital image correlation: from displacement measurement to identification of elastic properties—a review. *Strain* 2006;42(2):69–80.
- [11] Amodio D, Broggiato G, Campana F, Newaz G. Digital speckle correlation for strain measurement by image analysis. *Experimental Mechanics* 2003;43(4):396–402.
- [12] Ivanov D, Ivanov S, Lomov S, Verpoest I. Strain mapping analysis of textile composites. *Optics and Lasers in Engineering* 2009;47:360–70.
- [13] Fayolle X, Calloch S, Hild F. Controlling testing machines with digital image correlation. *Experimental techniques* 2007;31(3):57–63.
- [14] Bing P, Hui-min X, Tao H, Asundi A. Measurement of coefficient of thermal expansion of films using digital image correlation method. *Polymer Testing* 2009;28:75–83.
- [15] Motip, Technical specification art. nr. 04036, <www.motip.com>.
- [16] Hoffmann K. An introduction to measurements using strain gages. Darmstadt: Hottinger Baldwin Messtechnik GmbH; 1989.
- [17] European Committee for standardization, Eurocode 3: design of steel structures—part 1–2: general rules—structural fire design, rue de Stasart—B-1050 Brussels, Ref. No. EN 1993-1-2:2005; E.
- [18] Lindgren L. Finite element modeling and simulation of welding part 2: improved material modeling. *Journal of Thermal Stresses* 2001;24:195–231.
- [19] der Aa EV, Hermans M, Richardson I. Control of welding residual stress and distortion by the addition of a trailing heat sink. In: Cerjak H, Bhadeshia H, Kozeschnik E, editors. *Mathematical modelling of weld phenomena 8*. Technische Universität Graz; 2007. p. 1053–72.
- [20] Cunat P. Lassen van roestvast staal. In: *Materiaal en Toepassingen reeks*, vol. 3, 2007.
- [21] Mäkeläine P, Outinen J. Mechanical properties of an austenitic stainless steel at elevated temperatures. *Journal of Constructional Steel Research* 1998;46. [Paper no. 101].
- [22] Lecompte D, Smiths A, Sol H, Vantomme J, Hemelrijck DV. Mixed numerical-experimental technique for orthotropic parameter identification using biaxial tensile tests on cruciform specimens. *International Journal of Solids and Structures* 2007;44:1643–56.
- [23] Wattrisse B, Chrysochoos A, Muraccione J-M, Nemoz-Gaillard M. Analysis of strain localization during tensile tests by digital image correlation. *Experimental Mechanics* 2001;41:29–39.
- [24] Pan B, Asundi A, Xie H, Gao J. Digital image correlation using iterative least squares and pointwise least squares for displacement field and strain field measurements. *Optics and Lasers in Engineering* 2009;47:865–74.
- [25] Lava P, Cooreman S, Debruyne D. Study of systematic errors in strain fields obtained via dic using heterogeneous deformation generated by plastic fea. *Optics and Lasers in Engineering* 2010;48:457–68.
- [26] Schreier H, Braasch J, Sutton M. Systematic errors in digital image correlation caused by intensity interpolation. *Optical Engineering* 2000;39:2915–21.
- [27] Lava P, Cooreman S, Coppeters S, De Strycker M, Debruyne D. Assessment of measuring errors in dic using deformation fields generated by plastic fea. *Optics and Lasers in Engineering* 2009;47:747–53.